

## POLYMER-LIKE AND DIAMOND-LIKE CARBON COATINGS PREPARED BY RF-PECVD FOR BIOMEDICAL APPLICATIONS

G. E. STAN<sup>\*</sup>, D. A. MARCOV, A. C. POPA<sup>a, b</sup>, M.A. HUSANU

*National Institute of Materials Physics, P.O. Box MG-7, Bucharest-Magurele, 077125, Romania*

*<sup>a</sup>Army Center for Medical Research, CA Rosetti 37, 020012 Bucharest, Romania*

*<sup>b</sup>Department of Cellular and Molecular Medicine, Carol Davila University of Medicine and Pharmacy, Bucharest, Romania*

Hydrogenated amorphous carbon (a-C:H) films were grown by radio-frequency (1.78 MHz) plasma enhanced chemical vapour deposition technique onto medical grade Ti6Al4V substrates. By varying the deposition pressure (13.33 Pa and 53.33 Pa, respectively) and methane dilution (20% and 60%, respectively) several types of carbonic films were obtained, presenting different bonding structures, surface energies and morphological features reflected in their biological behaviour. FTIR, Raman, UV-Vis, XPS and AFM measurements were used for characterizing these structures. The surface energy was determined by contact angle measurements, and their thrombogenicity was tested by the activated partial thromboplastin time (aPTT) method. We have noticed that at the same values of methane in argon dilution but at different pressure values, the film structure was totally changed: soft polymer-like carbon (PLC) type at the higher pressure and hard diamond-like carbon (DLC) type at the lower pressure. Raman spectroscopy and XPS suggested that the highest  $sp^3$  ratio ( $\sim 52\%$ ), was found for DLC films prepared in a 60% methane dilution in argon. It has been found that for both PLC and DLC structures the surface energy has a decreasing tendency with the methane concentration increase in the deposition atmosphere. Excellent aPTT results were obtained for the DLC-60 ( $18.6 \pm 0.3$  min) and PLC-20 ( $17.4 \pm 0.5$  min) structures, superior to those recorded for Ti6Al4V and PMMA commercial materials. These values recommend the prepared carbonic structures for medical applications: harder coatings (DLC) for metal prostheses (heart valves, acetabular cups etc.), while softer and flexible coatings (PLC) for the textile vessels or stents biofunctionalization.

(Received June 30, 2010; accepted August 26, 2010)

*Keywords: Diamond-like carbon; Polymer-like carbon; RF-PECVD; Biomaterial; Surface energy; aPTT.*

### 1. Introduction

Hydrogenated amorphous carbon (a-C:H) structures represent a wide family of materials with a high potential for research and applications [1–4]. Their properties are mainly influenced by the hybridization state of the carbon atoms. Depending on the prevailing hybridization state one can speak about diamond-like films ( $sp^3$ ), graphitic films ( $sp^2$ ) and polymeric films ( $sp^1$ ) [5]. Such carbonic structures can be prepared by various methods such as ion beam deposition, magnetron sputtering, pulsed laser deposition and plasma enhanced chemical vapour deposition [6–9]. a-C:H films obtained by chemical deposition from gaseous hydrocarbons activated with the help of radio-frequency, microwave, and other types of plasmas, contain a significant quantity of hydrogen (as high as 50%) and could consist of several phases finely dispersed (diamond,

---

<sup>\*</sup>Corresponding author: george\_stan@infim.ro

graphite, and polymer phases). Diamond-like carbon (DLC) in particular is a candidate for biomedical applications due to its blood-compatibility and its excellent mechanical properties [4,9–10].

Radio-frequency plasma-activated enhanced chemical vapour deposition (RF-PECVD) allows the ease of tailoring different carbonic structures by varying the energy of the bombarding species upon the growing films. The implant-type coatings' surface energy values, roughness and bonding structures are important parameters for their biofunctionality. Usually a-C:H coatings are synthesized by RF-PECVD operating at high frequency (13.56 MHz) using as working atmosphere a hydrocarbon gas such as methane [11].

DLC coatings have an excellent haemocompatibility, which is expressed in a decreased thrombus formation. In general, the blood-compatibility of carbonic films, and moreover DLC films, is related to the fraction of  $sp^2$  bonds; the increase of  $sp^2$  content causes the retrogression of DLC haemocompatibility [12,13]. To the best of our knowledge there are no conclusive reports in relation to the thrombogenic properties of polymer-like films (PLC) deposited by RF-PECVD.

In the present work, a correlation between bonding structure and concentration of  $sp^3$ ,  $sp^2$  and  $sp^1$  hybridized carbon in a-C:H thin films and their physical-chemical and thrombogenic properties was attempted. Also a simple coating methodology for tailoring carbonic films' composition, based on RF-PECVD technique operating at low radio-frequency (1.78 MHz), was developed.

## 2. Experimental

### 2.1 Deposition of a-C:H coatings

The a-C:H structures were prepared in a coupled RF plasma CVD asymmetric reactor (UVN-75R1) driven by a 1.78 MHz power supply. Titanium biphasic alloy (Ti6Al4V – ASTM: F136) and glass (Corning 1737) were used as deposition substrates. Before loading into the chamber, the substrates (25 mm × 25 mm × 1 mm) were ultrasonically cleaned successively for 10 min in acetone and iso-propanol and dried by nitrogen purging. The substrates were fixed with silver paint onto the water-cooled RF cathode with a ~110 mm diameter.

The reactor was evacuated by a combination of a rotary mechanical and diffusion pump to a base pressure of  $\sim 10^{-4}$  Pa. Prior to deposition, the substrates were sputter cleaned for 10 min at a 0.4 kV DC bias voltage in argon plasma produced by a wolfram plasmatron in order to eliminate any impurity present on the substrate. These pre-treatments are also applied to improve the adhesion of the coatings to the substrates [14]. Subsequently, the chamber was again evacuated to  $10^{-4}$  Pa, and then the working gas was feed into the reactor.

The deposition parameters varied were the gas pressure (13.33 Pa and 53.33 Pa) and the working atmosphere composition (methane dilution in argon), the RF power being kept constant. The amorphous carbon a-C:H films were prepared in atmospheres of 60% and 20% methane dilution in argon. The mix gas flow rate was fixed at 45 sccm. When a RF power of ~100 W was supplied, the substrate temperature increased due to plasma bombardment, but it did not exceed 50°C, as monitored with a Chromel–Alumel thermocouple system. The self-bias voltage was measured, ranging from 335 to 400 V, depending on deposition conditions (Table 1). Carbonic coatings with a 300 nm thickness were deposited onto Ti6Al4V substrates for morphological analysis, physical-chemical characterization and biological testing, based on the deposition rates determined by Swanepoel method on a-C:H/glass coatings (Table 1).

Table 1. Deposition parameters for the a-C:H films synthesized by RF-PECVD.

Samples batch	Working atmosphere CH <sub>4</sub> :Ar (%)	Deposition pressure (Pa)	Gas flow (sccm)	DC <sub>bias</sub> (V)	Film type	Deposition rate (nm/min)
1 (PLC-20)	20:80	53.3 Pa	45	335	PLC	2.5
2 (PLC-60)	60:40	53.3 Pa	45	380	PLC	6
3 (DLC-20)	20:80	13.3 Pa	45	360	DLC	13.5
4 (DLC-60)	60:40	13.3 Pa	45	400	DLC	17

## 2.2 Spectroscopic measurements

The transmission measurements in UV–Vis range (10000–30000  $\text{cm}^{-1}$ ) were performed by using a PerkinElmer Lambda 90 UV–Vis–NIR spectrophotometer. The values of refractive index and a-C:H films' thicknesses were estimated by Swanepoel method [15] from the values and positions of maximum and minimum of the spectra in the low absorption region. This method offers a rigorous thickness determination of thin absorbing films on transparent substrates (glass in our case). The procedure allows calculating thicknesses with an accuracy of better than 1% [15].

Fourier Transform Infrared (FTIR) spectroscopy measurements were performed on a-C:H/Ti6Al4V samples by using a Perkin Elmer BX Spectrophotometer in Attenuated Total Reflectance (ATR) mode. We studied the absorption in the 2700–3100  $\text{cm}^{-1}$  range corresponding to the stretching band of C–H bonding, using a 2  $\text{cm}^{-1}$  resolution, with a total of 100 scans per experiment.

In order to thoroughly investigate the vibrations of the carbonic matrix Raman spectroscopy measurements were performed. A Renishaw 1000 micro Raman system, with a 30 mW Elforlight laser diode source operating at a wavelength of 532 nm, was used for all experiments.

The chemical bonding of carbon atoms ( $\text{sp}^3$ -,  $\text{sp}^2$ - or  $\text{sp}^1$ -hybridization) in the a-C:H films was investigated by X-ray photoelectron spectroscopy (XPS, Specs GmbH complex surface science setup, including a photoemission chamber) with Al  $K\alpha$  radiation and 20 eV pass energy applying C 1s line shape analyses. High resolution core level scans were acquired for the C 1s photoelectron peak. The deconvolution of the photoelectron peak was performed using spectra simulation based on the convolution of Lorentzian and Gaussian functions [16,17]. The spectra were recorded prior to sputter cleaning and after sputter cleaning for 10 minutes at a current of 10  $\mu\text{A}$  in order to analyze the ion-beam induced changes in the surface composition and bonding.

## 2.3 AFM topographical analysis

The topographical features ( $R_{\text{abs}}$ ,  $R_{\text{rms}}$ ) of the PLC and DLC coatings deposited onto titanium substrates were investigated by Atomic Force Microscopy (AFM). An A100-AFM microscope (A.P.E. Research, Italy) working in the non-contact mode in air at a 325 kHz resonance frequency, equipped with a commercial silicon cantilever (NSC15/AIBS, tip: radius < 10 nm; tip height 20–25  $\mu\text{m}$ , full tip cone angle < 30°), was used. AFM micrographs were recorded from different regions of the samples, using sampling areas of 30  $\mu\text{m} \times 30 \mu\text{m}$ . A low-pass filtering was performed in order to remove the statistical noise without loss of information. All AFM measurements were performed keeping the same conditions of room temperature and ambient atmosphere.

## 2.4 Surface energy estimation

The solid phase surface energy is an important characteristic of a material which has a direct influence on processes such wettability and cells' adhesion. The calculations of the solid surface energy performed were based on contact angle measurements, using standard solvents (water and ethylene glycol) with known surface tensions [18]. The surface energy measurements of the prepared a-C:H films were performed at 25°C by using a goniometric method, the two solvents being dropped onto surface and the contact angle estimated. The drops size and the drip distance were kept constant for each determination. The contact angle values determinations were made by the evaluation of the tangent angle of a sessile liquid drop on the a-C:H film solid surface, which is defined by the mechanical equilibrium of the drop under the action of three interfacial tensions: solid–vapour, solid–liquid and liquid–vapour, respectively. The surface energies were calculated using the Owens-Wendt approximation [19]. The experiments were performed in triplicate for each a-C:H surface. The statistical significance was determined using an unpaired Student's t-test. The differences were considered significant when  $p < 0.05$ .

## 2.5 Biological assays

In order to assess' interaction with blood coagulation systems we conducted a slightly modified protocol for manual detection of activated partial thromboplastin time (aPTT) described initially by J. Margolis: fresh blood was harvested in sodium citrate (3.2% final concentration) using Vacutainer medical devices from five healthy non-smoking patients. Samples were centrifuged 10 min at 2500 g and plasma from the five samples was pooled in order to minimize errors due to unknown pathology for a given volunteer.

Surfaces were cleaned with ethyl alcohol and ethyl ether and then dried at 25°C, for 2 h. Prior to test CaCl<sub>2</sub> was added to plasma to counter effects of sodium citrate and enable clotting. Samples were deposited on a plane surface and drops of plasma (50 µl) were deposited from a distance of 1 cm. The aPTT was considered as the time for plasma clotting on surface [20,21].

For comparison of prepared a-C:H (PLC and DLC type) characteristics with other biomaterials, the same analysis were performed on medical grade Ti6Al4V and poly(methyl methacrylate) (PMMA) plates. Five experiments were performed for each surface. The statistical significance was determined using an unpaired Student's t-test. The differences were considered significant when  $p < 0.05$ .

## 3. Results

### 3.1 Optical characterization

Independent of methane dilution the films deposited at higher pressures (53.33 Pa) were obtained transparent and soft (it could be easily scratched with a sharp-pointed needle showing a polymer-like character), while the films deposited at lower pressures (13.33 Pa) were obtained brownish and hard, qualities specific to DLC structures.

Transmission values around 100% are noticed for the PLC samples which are in agreement with the similar values of the refractive index for the glass substrate used (1.52) and PLC films (~1.45). The transmission of DLC films shows maxima and minima of interference in the region 4000–10000 cm<sup>-1</sup> and decreases due to the inter-band absorption at higher wave number values.

The absorption coefficient in the region of band to band absorption was used for estimating the value of Tauc optical gap using the representation:

$$(\alpha E)^{1/2} = B(E - E_0) \quad (1)$$

Where:  $E$  is the photon energy,  $E_0$  the optical gap and  $B$  a value proportional to the joint density of states. The optical gap display values around 1.5 eV for all the DLC films and a higher value of 4 eV for the PLC layer.

The films' deposition rates were determined by Swanepoel technique, described elsewhere [22,23]. One can notice that the a-C:H films' growth rate (Table 1) strongly depended on the methane fraction (20% and 60%) and the working gas pressures (13.33 Pa and 53.33 Pa), respectively. A dramatic decrease of deposition rate could be observed when increasing the working pressure. When the pressure increases, the number of ions generated in the plasma increases, resulting in a larger ion flux reaching the substrates. But higher atomic hydrogen concentration is also generated resulting in the etching of the growing films which can account for a decrease in the deposition rate as seen at higher pressure (53.3 Pa). Although the ion flux increases, the films' growth rate could not to be significant as at higher pressure the mean ion energy is expected to decrease with increasing pressure as a result of increased inelastic collision of the ions [24]. Therefore, the etching of the films by hydrogen is a dominant mechanism that accounts for the decrease of the deposition rate, affecting the growth of the films at higher pressure [24,25].

The growth rates are increasing with argon content decrease. This effect could be owned to the high carbon density concentration and thus to the increase of branching ratio of the CH<sub>n</sub> active

species. It is seen also that the films' thicknesses are monotonically increasing with the bias-voltage. This is in agreement with the previous assumption, the increase of the bias voltage is owned to an increase in the number of radicals which participate in the reaction, resulting in an enhanced ionization and dissociation of methane gas due to the increased electron energy in the plasma [26,27].

### 3.2 FTIR spectroscopy

FTIR measurements could provide information on the presence and concentration of hydrogen bonded to the carbon. The carbonic thin films were transparent in the IR range. Figure 1 display the absorption coefficient in the range 2700–3100  $\text{cm}^{-1}$  for the prepared DLC and PLC coatings. This region is characteristic for C–H stretch vibrations from  $\text{sp}^3$ - and  $\text{sp}^2$ -hybridized  $\text{CH}_n$ . All IR spectra showed a similar shape with a main broad peaked absorption band centred approximately at about 2920  $\text{cm}^{-1}$ . Seven vibrational components could be identified as distinct shoulders for the PLC and DLC samples: at 2823–2825  $\text{cm}^{-1}$  ( $\text{sp}^3$   $\text{CH}_2$  symmetric), 2864–2868  $\text{cm}^{-1}$  ( $\text{sp}^3$   $\text{CH}_3$  symmetric), 2919–2924  $\text{cm}^{-1}$  (superimposing of  $\text{sp}^3$   $\text{CH}_2$  asymmetric and  $\text{sp}^3$   $\text{CH}$  mode), 2957–2965  $\text{cm}^{-1}$  ( $\text{sp}^3$   $\text{CH}_3$  asymmetric), 3000–3004  $\text{cm}^{-1}$  ( $\text{sp}^2$   $\text{CH}$  olefinic), 3025–3026  $\text{cm}^{-1}$  ( $\text{sp}^2$   $\text{CH}_2$  olefinic) and 3058  $\text{cm}^{-1}$  ( $\text{sp}^2$   $\text{CH}_3$  aromatic) [28,29].

These C–H absorption bands are related only to carbon atoms bonded to one or more hydrogen atoms and do not reveal anything about the unbounded hydrogen in a-C:H network [30]. The difference between the absorption spectra of DLC and PLC films, in the range 2700–3100  $\text{cm}^{-1}$ , consists in the different intensities and widths bands values for the similar stretching lines. As an overall characteristic, the intensity of the stretching band is higher for the PLC coatings, denoting a higher concentration of bonded hydrogen atoms. Thus the intensity of these bands for PLC samples is related to the decrease in the  $\text{sp}^3$  fraction. A larger fraction of the  $\text{sp}^2$  phase and higher electron delocalization allows higher charge fluxes and thus higher IR activity [31]. The higher the concentration of  $\text{sp}^2$  phases the intenser the vibrational modes observed in the FTIR spectra. The increase in intensity of the main absorption peak in case of the higher deposition pressure is suggesting an increase of the reactive precursor gas dissociation, due to higher number of methane molecules collisions, in the growing films being incorporated more  $\text{sp}^2$  and  $\text{sp}^1$  hybridized carbon species.

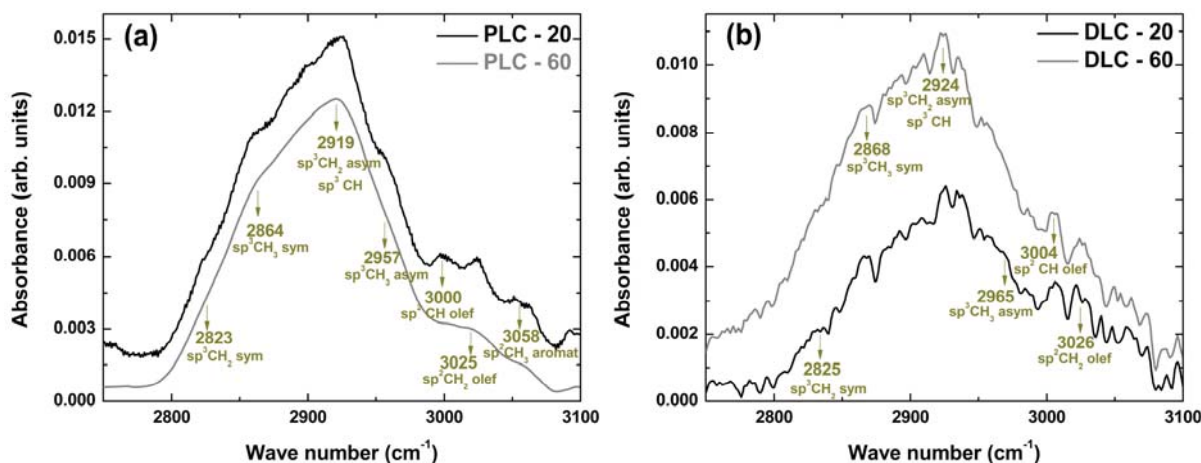


Fig. 1. FTIR spectra for PLC (a) and DLC (b) films prepared in 60%, respectively 20%  $\text{CH}_4$  dilution in argon atmosphere.

### 3.3 Raman investigation

Raman spectroscopy was used to characterize the quality of the DLC films obtained at different methane dilution, in terms of diamond carbon-phase purity (Figure 2). The spectra can be fitted using three Gaussian components. The DLC spectra contain typical broad peaks, the ‘G’ and ‘D’ peaks. The G-peak corresponds to the fundamental  $E_{2g}$  mode of graphite, and D-peak to disordered graphite [32]. The D band peaks for the two DLC films were positioned around  $1420\text{ cm}^{-1}$ , whereas, the G band peaks were centred at  $\sim 1590\text{ cm}^{-1}$ .

For the hard DLC films [33] the presence of a broad band between  $1100$  and  $1300\text{ cm}^{-1}$  is a fingerprint for the existence of diamond nanocrystals. In case a narrow peak at  $1332\text{ cm}^{-1}$  is evidenced, the diamond crystals have micrometric dimensions. Thus one can assume the presence of nanocrystalline diamond cluster with  $sp^3$ -bonding in the films. The position of the G peak and the ratio of the integrated areas under the D and G peaks ( $I_D/I_G$ ) can be correlated with the  $sp^3/sp^2$  bonding ratio [34,35]. Increases in the  $I_D/I_G$  ratio, the shifting of the G peak towards higher wave numbers and widening of the D-peak are indicating in general the increase of the graphite-like concentration in the amorphous carbon films [36–38].

One can notice that the value of  $I_D/I_G$  ratio is lower for the higher methane concentration, which corresponds to a maximum percent of  $sp^3$ -C bonds [33]. The increase in the  $sp^3$  content of the DLC-60 films is probably owned to the presence of more atomic hydrogen at higher methane content which preferentially impinge the graphitic  $sp^2$ -components in the growing films. S. Zhang et. al. [37,39] showed that the  $sp^3$  fraction is inversely proportional to the band ratio  $I_D/I_G$ . Thus, one can expect that the highest  $sp^3$ -C bonds concentration is obtained for the DLC structures prepared in 60% methane in argon dilution.

Moreover, the position of G peak shifts from  $1587.3$  to  $1590.1\text{ cm}^{-1}$  (see Figure 2-a,b, Table 2) with the increase of argon content. In principle, in the Raman spectra of carbon based materials the G-peak positions move to higher wave number due to two processes: the high  $sp^2$  content or cluster size and due to higher compressive stress [40]. As seen in Figure 2-a,b the FWHM of D-peak also showed an increase for DLC-20, which is in agreement with the above assumptions (Table 2).

In DLC, graphene regions of  $sp^2$  carbons are heavily conjugated, at the boundaries of graphene regions appearing partial charges which could promote adsorption of charged blood proteins such as coagulation factors, kininogens etc. Therefore the more boundaries of graphene regions or more distorted graphene regions we have, the more partial charges will appear, and the faster proteins will adsorb and the faster blood / plasma will coagulate.

Table 2.  $I_D$  and  $I_G$  Raman values for the DLC-20 and DLC-60 samples.

Sample	$I_D/I_G$	FWHM D peak ( $\text{cm}^{-1}$ )	Working atmosphere $\text{CH}_4:\text{Ar}$ (%)	D peak position ( $\text{cm}^{-1}$ )	G peak position ( $\text{cm}^{-1}$ )
DLC-20	0.4778	238.5	20:80	1433.3	1590.1
DLC-60	0.4369	235.9	60:40	1411.2	1587.3

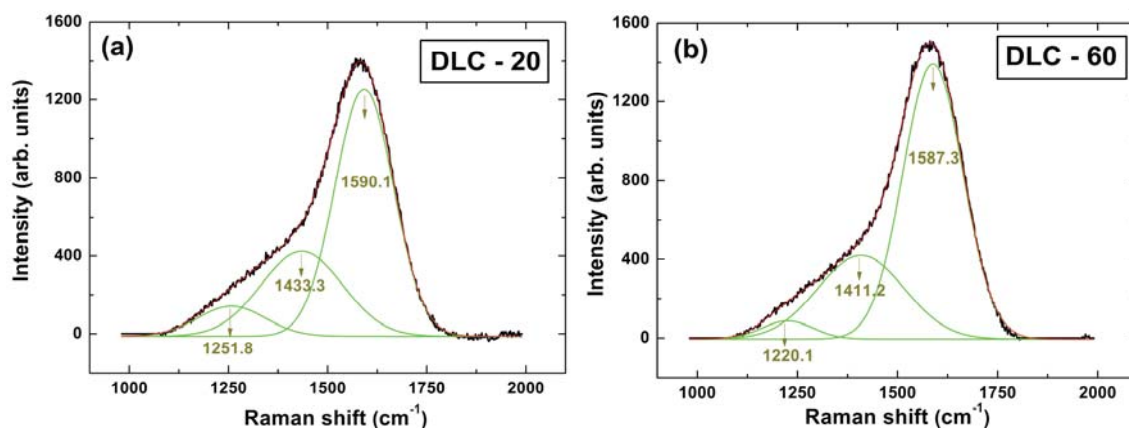


Fig. 2. Raman spectra corresponding to a-C:H films prepared in: a) DLC-20; b) DLC-60.

### 3.4 XPS characterization

The measured C 1s spectra were deconvoluted as shown in Figure 3. The photoelectron spectra showed very complex shapes indicating the existence of different chemical states for C 1s. From deconvolution studies, was evident that three contributions should be taken into account for the C 1s peak in case of PLC sample due to  $sp^1$ ,  $sp^2$  and  $sp^3$ -C hybridizations. The deconvolution studies of the C 1s spectra in case of DLC samples revealed two synthetic distinct peaks assignable to  $sp^2$  and  $sp^3$ -C hybridizations. The peak situated a higher binding energy (BE) is assigned to  $sp^3$  bonded carbon (C-C and C-H), and those at lower BE correspond to  $sp^2$  and  $sp^1$ , respectively, hybridization states of carbon. The FWHM of the  $sp^3$  peak was in 1.5–2.5 eV range for all samples (Figure 3 and Table 3).

The absence of the inelastic tail associated with the  $sp^2$  and  $sp^1$  components suggests that the XPS signal is related with the outer atomic layers, while the  $sp^3$  component, featured by an inelastic tail in their XPS spectrum, are associated with atomic layers located below the  $sp^2$ - $sp^1$  layer [16,41]. The content of  $sp^3$ ,  $sp^2$ , and  $sp^1$  carbon in all the investigated films was evaluated from their corresponding peaks' area. The measured areas of  $sp^3$ ,  $sp^2$ , and  $sp^1$  carbon components are presented in Table 3.

At the lower working pressure one can notice a higher content of  $sp^3$ -C in case of the films prepared at the 60% methane dilution (DLC-60). The result is in agreement with the FTIR and Raman measurements which suggested a lower content of  $sp^2$  for these films. The samples deposited at the higher pressure presented comparable amounts of  $sp^2$ -C (~55%). At the higher pressure and 20% methane dilution (PLC-20 samples) lower content of  $sp^1$  (~17 %) and a higher content of  $sp^3$  (~28%) was obtained. When increasing the methane dilution (PLC-60), the  $sp^1$ -C concentration increases (~33%) and the  $sp^3$ -C concentration strongly decreases (~7%). It is suggested that at higher argon pressure and larger methane dilution in argon atmosphere, the degree of active molecules dissociation is enhanced, due to higher number of collisions, into the growing carbonic films being incorporated more  $sp^2$  and  $sp^1$  hybridized carbon species.

Table 3.  $sp^3$ -,  $sp^2$ - and  $sp^1$ -C concentration calculated from XPS spectra deconvolution.

Sample	$sp^3$ -C component (%)	$sp^2$ -C component (%)	$sp^1$ -C component (%)	FWHM $sp^3$ -C peak (eV)
PLC-20	27.73	54.85	17.42	2.03
PLC-60	7.83	59.55	32.62	2.85
DLC-20	48.75	51.25	-	1.73
DLC-60	51.63	48.37	-	1.75

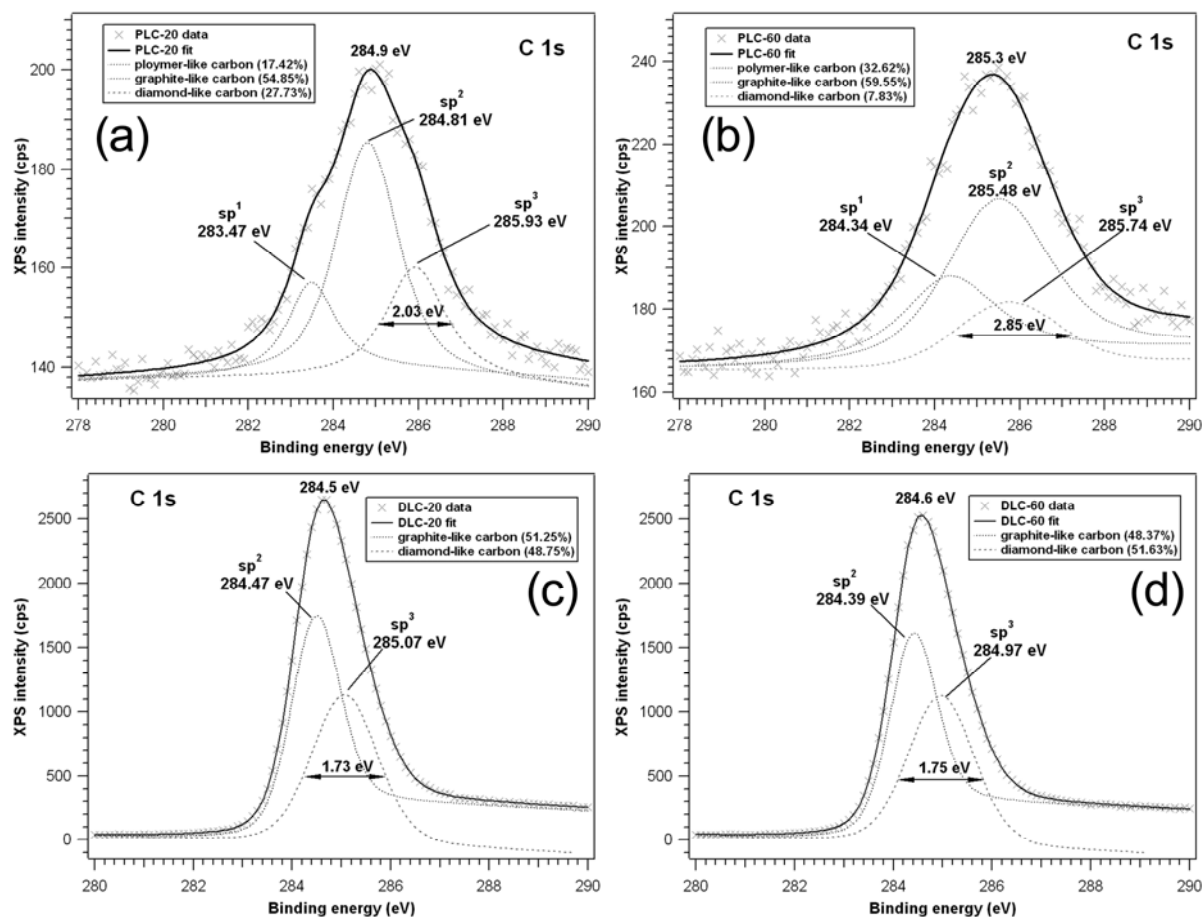


Fig. 3. High resolution XPS spectra for C 1s core level photoelectron after sputter cleaning: (a) PLC-20; (b) PLC-60; (c) DLC-20 and (d) DLC-60.

### 3.5 AFM analysis

Figure 4 displays the AFM images for the two types of carbonic structures. The 3D topographic AFM images revealed homogeneous surfaces with a very low variation of colour and contrast, which demonstrate that both types of structures are relatively smooth (Figure 4). As a general observation, the shape and features of functional carbonic structures are following the features of the substrates' surfaces. An  $R_{\text{rms}}$  value of  $\sim 117$  nm was found for the Ti6Al4V substrates. Considering this, along with the results recorded on the samples deposited on glass (Figure 4), which gave  $R_{\text{rms}}$  values lower than 6 nm, than both types of films are rather smooth with  $R_{\text{rms}}$  values ranging from 94 to 120 nm roughness. The AFM micrographs recorded on a-C:H/glass structures revealed smooth and fine PLC and DLC films, optimal for haemocompatible applications [10,42]. However, one can notice important differences in the height and diameter values of the surface peaks. These values are more homogeneous for the PLC films in comparison to the DLC ones.



Fig. 4. AFM 3D topographic images for: (a) Ti6Al4V substrate; (b,c) PLC coatings and (d,e) DLC coatings.

### 3.6 Surface energy measurements

Lower surface energy values have been determined for the DLC coatings (Table 4). One can notice a decrease of the surface energy with the methane dilution increase for both types of structures. The surface energy values recorded for DLC coatings are lower than those of Ti6Al4V and medical grade poly(methyl-methacrylate) (PMMA) substrates. The PLC coatings' surface energy is comparable with that of PMMA.

The two tailed t-testing, assuming unequal variances, showed statistically significant differences between the surface energy values of the PLC-60, DLC-20, and DLC-60 structures with respect to those of the Ti6Al4V and PMMA samples ( $p < 0.05$ ). No statistical significant differences were found in case of PLC-20 samples compared to the PMMA bare substrates ( $p=0.39 > 0.05$ ).

Table 4. Surface energy results for PLC and DLC samples in comparison with the Ti6Al4V alloy substrates and commercial polymer materials.

Sample batch	Surface energy (mN/m)
PLC-20	35.84±0.47
PLC-60	34.22±0.52
DLC-20	31.96±0.75
DLC-60	30.23±0.63
Ti6Al4V	37.85±0.94
PMMA	36.35±0.78

### 3.7 aPTT results

Blood coagulation is initiated via two major mechanisms: contact activation pathway and tissue factor pathway. In case of contact activation pathway, collagen from the blood vessel binds Factor XII, prekallikrein and high molecular weight kininogen (HMWK). In this complex, prekallikrein is converted to kallikrein and factor XII is activated. The activated Factor XII starts the coagulation cascade which ends with formation of the fibrin clot. The partial thromboplastin time (PTT) is generally used to detect the activation degree/abnormalities in contact activation pathway of the coagulation system, and in the manual method implies adding to the blood/plasma sample an activator such as silica, kaolin, celite or ellagic acid [20,21]. In our experiment we used as activator the surface of our deposited materials or medical grade materials. The maximum value for the thromboplastin time was recorded for the DLC structures prepared in 60% methane atmosphere, superior to those of Ti6Al4V and PMMA commercial material (Table 5). By comparison with Ti6Al4V, the contact with the DLC-60 coated surfaces suppresses the activation of the endogenous clotting system. The phenomenon could be explained by a poor addition of plasma proteins to the film, and a decreased onset of coagulation cascade. Also a preferential albumin adsorption on materials' surface might inactivate it for blood clotting. Interestingly excellent aPTT times were also obtained for the PLC-20 samples (17.4 min), better than those for recorded for the DLC-20 coatings (16.2 min). The two tailed t-testing, assuming unequal variances, showed statistically significant differences between the PLC-20, DLC-20, and DLC-60 aPTT results obtained with respect to the Ti6Al4V and PMMA samples ( $p < 0.05$ ). No statistical significant differences were found in case of PLC-60 samples compared to the Ti6Al4V bare substrates ( $p=0.09 > 0.05$ ).

Table 5. Thromboplastine results for PLC and DLC samples in comparison with the Ti6Al4V alloy substrates and commercial PMMA materials.

Sample	Activated partial thromboplastine time (min)
PLC-20	17.4±0.5
PLC-60	14.2±0.4
DLC-20	16.2±0.8
DLC-60	18.6±0.3
Ti6Al4V	13.4±0.8
PMMA	15.0±0.6

#### 4. Discussion

It is now well known that the ability of carbon to form different bonding configurations is responsible for the wide range of properties of amorphous carbon films: mechanical, tribological, electrical and biological. In particular, the ratio of diamond ( $sp^3$ ) / graphite ( $sp^2$ ) is often cited as the controlling factor for both the mechanical and biological properties, but few data about the optimal  $sp^3/sp^2$  ratio were published. Moreover the implications of  $sp^1$  hybridized carbon concentration in a-C:H films on their biological behaviour were not yet discussed.

The content of  $sp^3$  hybridization state of carbon plays a defining role in the mechanical properties of the biofunctional coating. Its optimal value depends on the medical applications: the coating should be harder for metal prostheses (heart valves, etc.), while for the textile vessels or stents, the coatings should be flexible and softer (larger concentration of  $sp^2$  or  $sp^1-C$ ) [43]. This is why we have also studied PLC coatings as a possible candidate biomaterial.

By varying the RF-PECVD deposition parameters, we have observed that it is easy to tailor the carbonic coatings' composition. The influence of the working atmosphere and pressure on the chemical bonding structure, surface energy and aPTT time was studied. It has been noticed that at the same values of methane dilution in argon and similar  $DC_{bias}$  but at different pressure values, the film structure was totally changed: polymeric type at the higher pressure values (53.3 Pa) and diamond type at the lower pressure (13.3 Pa). The increase of the deposition pressure enhances the bombardment of the energetic ions which are modifying the structure and the properties of the film by breaking off weak bonds and trapped gas molecules. When the methane dilution is increased, the bias voltage is increasing as well, which suggests that a larger number of radicals participate in the reaction, resulting in an enhanced ionization and possible further dissociation of methane gas of other already ionized molecules, due to the increased electron energy in the plasma. Thus, at the higher pressure the number of molecules collisions is increasing, the larger the methane content the more enhanced is the active molecules' dissociation. The presence of  $sp^2-$  and  $sp^1-C$  in the PLC films could be explained by the active removal of bound hydrogen from the films' surface during the growth process. For the lower pressure the increase of methane content is leading to high content of methyl ( $CH_3-$ ) groups in the film which appear as a possible consequence of the dissociation of methane molecules by electron impact.

For both types of carbonic coatings the tendency of the surface energy is to decrease, along with the increasing of the methane concentration in deposition atmosphere (Tables 4 & 5). One can notice that for DLC structures the tendency of the partial thromboplastin time is to increase with the  $sp^3-C$  concentration and the decrease of surface energy values. Lower values of the surface energy were observed for the carbonic coatings with higher roughness (Table 4 & Figure 4).

Both PLC structures contain a high amount of  $sp^2$  (~60%) and a significant proportion of  $sp^1$  (17–33%) in contrast to DLC ones. Also correlating this data with the FTIR information, which sustains a bigger number of C–H bonds in PLC structures, it is obvious that  $sp^2$  carbons in PLC would rather form long chains with double bonds than organizing in graphene structures which lack hydrogen. We can propose that due to the fact that ~60% of C atoms are  $sp^2$  hybridized, many carbon atoms are involved in alternating double/single C–C bonds which are supposed to

conjugate. Conjugation is a process in which  $\pi$  orbitals are distorted, electrons are unevenly distributed and promotes apparition of partial charges, which conduct to a higher hydrophilic character and higher interaction with ions present in plasma and with charged proteins leading to a better adsorption to surface. In this type of structures two carbon double bonds close one to each other are the end of conjugation zone. Also a “stop” signal for conjugation is represented by two simple C–C bonds. A  $\text{CH}_3$ - side chain (with a  $\text{sp}^3$  carbon) on a long chain with alternating double and simple C–C bonds, would not stop the conjugation process. Therefore in the case of PLC-20, where we have large amounts of  $\text{sp}^3$  and small amounts of  $\text{sp}^1$  (number which acts as a stop for conjugation), the length of the conjugating chain would longer resulting a small number of partial charges to the number of carbon atoms involved. Therefore when there are fewer (but longer) chains that conjugate the smaller density of partial charges would appear decreasing adsorption of blood proteins and decreasing coagulation. This would explain the smaller times for coagulation for PLC-60 than for PLC-20. The properties of PLC vary greatly with concentrations of  $\text{sp}^3$  and  $\text{sp}^1$ , which can be modulated easily by changing RF-PECVD deposition parameters. It is our hope that by a fine adjusting of deposition parameters it should be possible to modulate the films' features and obtain the carbonic structures with optimal properties (long coagulation time and elevated plasticity).

## 5. Conclusions

We have prepared amorphous hydrogenated carbon structures by RF-PECVD (1.78 MHz) in two atmospheres of methane diluted in argon (20% and 60%, respectively). Diamond-like carbon films have been obtained at 13.3 Pa pressure and polymer-like carbon films at 53.33 Pa. The DLC structures with the highest  $\text{sp}^3$  carbon atoms concentration ( $\sim 52\%$ ), corresponding to a minimum value of the  $I_D/I_G$  ratio, were obtained for the 60% methane dilution. A further increasing of the deposition pressure, keeping the same methane dilutions, drastically changed the character of the carbonic films from DLC to PLC. The highest  $\text{sp}^1$ -C content was obtained for the PLC-60 coatings. The refractive index dropped from 2.05 (DLC) to 1.41 (PLC), while the optical gap increased from 1.51 eV to around 4 eV. Small topographic modifications accompanied changes in structure as seen in AFM images. Coagulation times (aPTT) of different a-C:H coatings varied widely with the bonding states of carbon present in the film. Promising aPTT results were obtained in case of DLC-60 (18.6 min) and PLC-20 (17.4) structures, superior to those recorded on medical grade materials. Further insightful biological tests are intended in order to fully evaluate the potential of these coatings for biomedical applications.

## Acknowledgements

GES and DAM want to express their gratitude to their scientific coordinator, Dr. Constantin-Octavian Morosanu, who sadly passed away in 2009 after a long and painful sufferance. Authors also thank Dr. Cristian-Mihail Teodorescu for the professional assistance with XPS measurements. The financial support of Core Program – Contract PN09-45 is acknowledged.

## References

- [1] J. Fontaine, T. Le Mogne, J.L. Loubet, M. Belin, *Thin Solid Films* **482**, 99 (2005).
- [2] R. J. Narayan, *Int. Mater. Rev.* **51**, 127 (2006).
- [3] M. Vojs, E. Zdravecka, M. Marton, P. Bohac, L. Franta, M. Vesely, *Microelectron. J.* **40**, 650 (2009).
- [4] X. Ye, Y. Shao, M. Zhou, J. Li, L. Cai, *Appl. Surf. Sci.* **255**, 6686 (2009).
- [5] J. Ristein, R. T. Stief, L. Ley, W. Beyer, *J. Appl. Phys.* **84**, 3836 (1998).
- [6] B. Druz, I. Zaritskiy, J. Hoehn, V. I. Polyakov, A. I. Rukovishnikov, V. Novotny, *Diam. Relat. Mat.* **10**, 931 (2001).

- [7] N. Paik, Surf. Coat. Technol. **200**, 2170 (2005).
- [8] J. Eskusson, R. Jaaniso, E. Lust, Appl. Phys. A-Mater. Sci. Process. **93**, 745 (2008).
- [9] F. R. Marciano, L. F. Bonetti, L. V. Santos, N. S. Da-Silva, E. J. Corat, V. J. Trava-Airoldi, Diam. Relat. Mat. **18**, 1010 (2009).
- [10] G. Dearnaley, J. H. Arps, Surf. Coat. Technol. **200**, 2818 (2005).
- [11] G. Fedosenko, A. Schwabedissen, D. Korzec, J. Engemann, Surf. Coat. Technol. **142–144**, 693 (2001).
- [12] M. Jelínek, K. Smetana, T. Kocourek, B. Dvořánková, J. Zemek, J. Remsa, T. Luxbacher, Mater. Sci. Eng. B-Solid State Mater. Adv. Technol. **169**, 89 (2010).
- [13] G. E. Wnek, G. L. Bowlin, Encyclopedia of Biomaterials and Biomedical Engineering, 1<sup>st</sup> ed., volume 3, Informa Healthcare, New York (2004).
- [14] G. E. Stan, C. O. Morosanu, D. A. Marcov, I. Pasuk, F. Miculescu, G. Reumont, Appl. Surf. Sci. **255**, 9132 (2009).
- [15] R. J. Swanepoel, J. Phys. E: Sci. Instrum. **16**, 1214 (1983).
- [16] D. Mardare, D. Luca, C. M. Teodorescu, D. Macovei, Surf. Sci. **601**, 4515 (2007).
- [17] C. M. Teodorescu, J. M. Esteva, R. C. Kainatak, A. El Afif, Nucl. Instrum. Methods Phys. Res. Sect. A-Accel. Spectrom. Dect. Assoc. Equip. **345**, 141 (1994).
- [18] <http://www.surface-tension.de/>
- [19] D. K. Owens, R. C. Wendt, J. Appl. Polym. Sci. **13**, 1741 (1969).
- [20] J. Margolis, J. Clin. Pathol. **11**, 406 (1958).
- [21] D. L. McGlasson, R. L. Brey, D. M. Strickland, W. R. Patterson, Clin. Lab. Sci. **2**, 109 (1989).
- [22] J. Sanchez-Gonzalez, A. Diaz-Parralejo, A.L. Ortiz, F. Guiberteau, Appl. Surf. Sci. **252**, 6013 (2006).
- [23] G. E. Stan, D. Bojin, U.P.B. Sci. Bull. Series B **72**, 187 (2010).
- [24] Y. T. Kim, S. M. Cho, W. S. Choi, B. Hong, D. H. Yoon, Surf. Coat. Technol. **169-170**, 291 (2003).
- [25] Y. H. Cheng, Y. P. Wu, J. G. Chen, X. L. Qiao, C. S. Xie, B. K. Tay, S. P. Lau, X. Shi, Surf. Coat. Technol. **135**, 27 (2000).
- [26] B. G. Choi, J. K. Kim, W. J. Yang, K. B. Shim, J. Ceram. Process. Res. **6**, 101 (2005)
- [27] G. J. Vandendentop, M. Kawasaki, R. M. Nix, I. G. Brown, M. Salmeron, G. A. Somorjai, Phys. Rev. B **41**, 3200 (1990).
- [28] G. Lazar, K. Zellamaa, I. Vascan, M. Stamate, I. Lazar, I. Rusu, J. Optoelectron. Adv. Mater. **7**, 647 (2005).
- [29] G. Socrates, Infrared and Raman Characteristic Group Frequencies—Tables and Charts, John Wiley & Sons Ltd. (2007).
- [30] L. Valentini, J. M. Kenny, G. Mariotto, P. Tosi, J. Mater. Sci. **36**, 5295 (2001).
- [31] M. Bonelli, A. C. Ferrari, A. Fioravanti, A. Li Bassi, A. Miotello, P. M. Ossi, Eur. Phys. J. B **25**, 269 (2002).
- [32] M. J. Jackson, W. Ahmed, Surface Engineered Surgical Tools and Medical Devices, Springer – Medical, 581 pages, (2007).
- [33] J. Schwan, S. Ulrich, V. Batori, H. Ehrhardt, S. R. P. Silva, J. Appl. Phys. **80**, 440 (1996).
- [34] C. Liu, D. Hu, J. Xu, D. Yang, Min Qi, Thin Solid Films **496**, 257 (2006).
- [35] S. S. Tincheva, Y. Dyulgerska, P. Nikolova, D. Grambole, U. Kreissig, T. Z. Babeva, J. Optoelectron. Adv. Mater. **8**, 308 (2006).
- [36] I. Ahmad, S. S. Roy, Md. A. Rahman, T. I. T. Okpalugo, P. D. Maguire, J. A. McLaughlin, Curr. Appl. Phys. **9**, 937 (2009).
- [37] S. Zhang, X. T. Zeng, H. Xie, P. Hing, Surf. Coat. Technol. **123**, 256 (2000).
- [38] M. G. Beghi, A. C. Ferrari, C. E. Botani, A. Libassi, B. K. Tanner, K. B. K. Teo, J. Robertson, Diamond Relat. Mater. **11**, 1062 (2002).
- [39] A. Zeng, E. Liu, P. Hing, S. Zhang, S. N. Tan, I. F. Annergren, J. Gao, Int. J. Mod. Phys. B **16**, 1024 (2002).
- [40] J. K. Shin, C. S. Lee, K. R. Lee, K. Y. Eun, Appl. Phys. Lett. **78**, 631 (2001).

- [41] D. Luca, C.M. Teodorescu, R. Apetrei, D. Macovei, D. Mardare, *Thin Solid Films* **515**, 8605 (2007).
- [42] T. Hasebe, T. Ishimaru, A. Kamijo, Y. Yoshimoto, T. Yoshimura, S. Yohena, H. Kodama, A. Hotta, K. Takahashi, T. Suzuki, *Diamond Relat. Mater.* **16**, 1343 (2007).
- [43] T. Kocourek, M. Jelinek, V. Vorlíček, J. Zemek, T. Janča, V. Žížková, J. Podlaha, C. Popov, *Appl. Phys. A-Mater. Sci. Process.* **93**, 627 (2008)